The effect of flow maldistribution in heterogeneous parallel-plate active magnetic regenerators

Nielsen, Kaspar Kirstein; Bahl, Christian; Engelbrecht, Kurt

Published in:
Journal of Physics D: Applied Physics

Link to article, DOI:
10.1088/0022-3727/46/10/105002

Publication date:
2013

The effect of flow maldistribution in heterogeneous parallel-plate active magnetic regenerators

K.K. Nielsen, C.R.H. Bahl and K. Engelbrecht
DTU Energy Conversion
Technical University of Denmark
Frederiksborgvej 399, DK-4000 Roskilde, Denmark
kaki@dtu.dk

Abstract. The heat transfer properties and performance of parallel plate active magnetic regenerators (AMR) with heterogeneous plate spacing are investigated using detailed models previously published. Bulk heat transfer characteristics in the regenerator are predicted as a function of variation in plate spacing. The results are quantified through a Nusselt number scaling factor that is applied in a detailed 1D AMR model. In this way, the impact of flow maldistribution due to heterogeneous parallel plate stacks on AMR performance is systematically investigated.

It is concluded that parallel plate stacks having a standard deviation greater than about 5 % on their plate spacing are severely penalized in terms of both cooling power and achievable temperature span due to the inhomogeneity of the stacks. Keywords: Flow maldistribution; Active magnetic regenerator; parallel plate heat exchanger; magnetocaloric effect; magnetic refrigeration

1. Introduction

The active magnetic regenerator (AMR) principle is applied in refrigeration cycles based on one or multiple solid magnetocaloric materials [1]. The magnetocaloric effect (MCE) is present in ferromagnets and may be manifested as an adiabatic temperature change or isothermal entropy change upon varying an applied magnetic field under the respective conditions. The effect is typically around a few degrees at an applied field of 1 tesla and varies significantly between materials [2, 3]. In order to achieve temperature spans larger than the MCE the AMR principle is applied. Here, the magnetocaloric solid both delivers the work input, through the MCE, and stores the achieved temperature gradient thus acting as a thermal regenerator.

The AMR principle is realized by organizing the magnetocaloric solid in an open porous structure through which a heat transfer fluid may flow. Such structures may be designed in different ways including packed particles (e.g. spheres), parallel plates, stacked wire mesh screens or extruded honeycomb-like structures [4, 5, 6, 7].

The two most important parameters associated with a regenerator from a performance stand-point are the flow resistance and heat transfer rate at a given set of relevant operating conditions. Other parameters such as compactness due to limited space in high magnetic field regions and demagnetizing effects are also important for AMRs [8, 9]. An example of a regenerator matrix geometry that theoretically promises a sufficient compromise between the flow resistance and heat transfer performance is based on flat parallel plates. Decreasing the channel size (distance between adjacent plates) increases the heat transfer coefficient, and decreasing the plate thickness makes the regenerator more compact and increases the specific surface area while maintaining the flow resistance at a tolerable level for application as an AMR [10, 11].

However, experimentally parallel plate AMRs have not been proven to perform as predicted by advanced models [12, 13, 14]. Similarly, in other related heat transfer applications applying parallel plate heat exchangers with flow channel hydraulic diameters in the micro regime, the experimentally determined performance is significantly smaller than theoretically predicted [15]. Here, micro channels are defined as having hydraulic diameters less than 1 mm, which for parallel plates means a plate spacing of maximum 0.5 mm.

Recently it has been suggested that inhomogeneity in a stack of parallel plates may lead to severe performance degradation [16, 17, 20]. If the thickness of the individual channels varies the channels will experience different flow rates. This leads to deviations from theoretical models that typically assume periodic regenerators [12]. They cannot therefore capture the effects present in heterogeneous stacks.

Given a stack of parallel plates, which are spaced randomly within certain limits, each individual channel will experience a different flow rate if the pressure drop across each channel is assumed equal. This is a function of the overall stack configuration and the individual channel thickness. The variation in flow channel thickness implies significantly larger flow rates in larger channels and likewise reduced flow rates in the

smaller channels. This is seen from the mean fluid velocity in the ith channel [17]

$$\tilde{u}_i = \dot{V}' \frac{H_{\mathrm{f},i}^2}{\sum_{j=1}^{j=N} H_{\mathrm{f},j}^3}, \tag{1}$$

where $\dot{V}'$ is the total volumetric flow rate per unit width of the stack, $H_{\mathrm{f},i}$ is the thickness of the ith channel and N is the total number of channels in the stack.

Recalling the definition of the Nusselt number

$$\mathrm{Nu} = \frac{h d_h}{k_\mathrm{f}}, \tag{2}$$

where h is the convective heat transfer coefficient, d_h the hydraulic diameter and k_f the thermal conductivity of the fluid. For parallel plates in contact with an aqueous heat transfer fluid the Nusselt number is nearly constant [18]. It is seen that larger channels have a smaller value of h than thinner channels have (since $d_h = 2H_\mathrm{f}$ where H_f is the channel thickness). Thus, the channels with poorer heat transfer performance receive the largest amount of flow in a heterogeneous parallel plate stack. This effect will decrease the overall performance of the stack compared to a homogeneous stack. Furthermore, the bulk heat transfer performance is sensitive to the ordering of the stack and will generally vary with the distribution of the channels - even though the same set of channel thicknesses are considered [20].

1.1. Regenerator geometry

The method for quantifying the reduction of the heat transfer coefficient applied was based on 50 stacks of parallel plates each containing 20 normally distributed flow channels [17, 20]. By carefully comparing the output temperature profile of the stacks to that of a single channel, and thus per definition homogeneous model, it was possible to extract a Nusselt-number scaling factor, $\mathrm{Nu_{scl}}$. This factor was found to be a function of flow rate, thermal and geometric properties of the stack. It represents a scaling of the Nusselt number such that the heat transfer coefficient effectively is decreased when $\mathrm{Nu_{scl}} < 1$ and increased when $\mathrm{Nu_{scl}} > 1$

In Refs. [17, 20] the details behind the derivation of the $\mathrm{Nu_{scl}}$ factor are provided. The technique applied uses certain properties of the fluid outlet temperature as a function of time (see, e.g., Ref. [21] for details). In this case the difference in time of the breakthrough of the temperature outlet curve at 20 and 80 %, respectively, is applied. This value is compared to that of the outlet curve of a single channel model where the thermal contact between the solid plate and the heat transfer fluid is varied. Effectively, this decreases the heat transfer coefficient of the ideal single channel model and it is thus possible to find the bulk heat transfer coefficient in the heterogeneous model.

In Fig. 1 the channel thicknesses of one of these 50 stacks are provided for the five standard deviation values. The figure shows that due to the random nature of the plate spacings there will be situations where, e.g., two channels with thicknesses larger than the average are adjacent in which case the plate between the two channels will

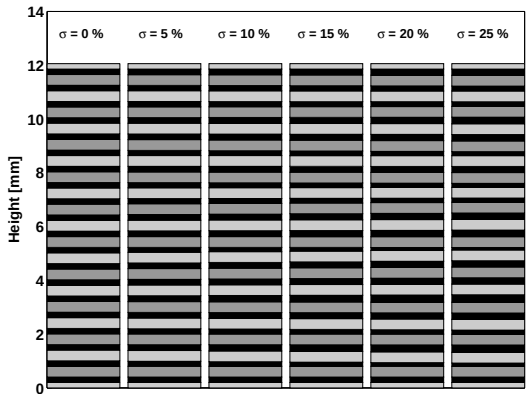

Figure 1. Cross sections of one of the 50 normally distributed stacks considered. Six standard deviations, as indicated at the top of the figure, are considered. The flow channels are colored black while the solid plates are colored grey in two alternating nuances in order to make the figure clearer.

experience significantly less heat transfer than plates located around smaller channels. At the same time a larger amount of the total fluid flow occurs in the larger channels and the heat exchanger thus experiences two simultaneous effects that will have an overall negative impact on the heat transfer performance.

In this paper an established 1D numerical AMR model [19] is used to quantify the influence on AMR performance due to inhomogeneity of the stack. The Nusselt number scaling factor ($\mathrm{Nu_{scl}}$) is applied as a function of Reynolds number in the model. The details are discussed in Sec. 2. The model is applied to a range of parameter configurations and the results are presented and discussed in Sec. 3. Finally, in Sec.4 the paper is concluded.

2. Numerical models

2.1. Flow maldistribution

A two-dimensional numerical heat transfer model of heterogeneous parallel plate stacks was developed in Refs. [16, 17, 20]. For analyzing the heat transfer performance of such a stack the model is applied in a single blow mode. Here, the solid plates and the fluid in the flow channels are initiated at a temperature, T_{init}, and at time 0 s fluid is moved into the flow channels at one end with a temperature different from T_{init}. At the opposite end (the outlet) the fluid exits and the outlet temperature is thus found as a function of time. An example of such a curve is given in Fig. 2(a).

The model solves the coupled, transient partial differential equations governing heat transfer by conduction and convection in the fluid and the solid. These may be expressed as

$$\rho_{\mathrm{f}} c_{\mathrm{f}} \left(\frac{\partial T_{\mathrm{f}}}{\partial t} + \mathbf{u} \cdot \nabla T_{\mathrm{f}} \right) = k_{\mathrm{f}} \nabla^2 T_{\mathrm{f}} \tag{3}$$

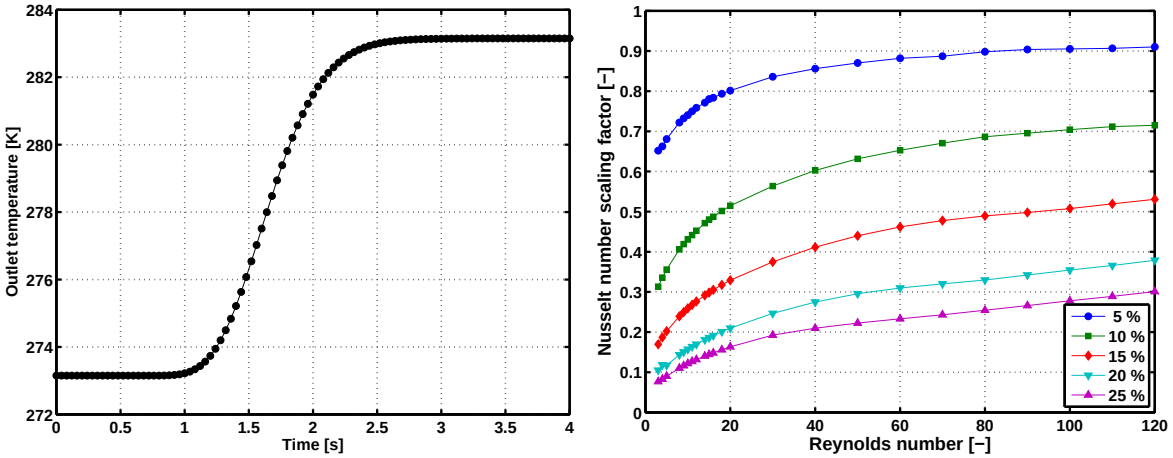

(a) (b)

Figure 2. (a) an example of a temperature outlet curve from the heterogeneous plate model. The initial temperature was set to 273 K and the inlet temperature to 283 K. (b) the Nusselt number scaling factor as a function of Reynolds number (based on results from Ref. [20]). The legend indicates the standard deviation of the normally distributed parallel plate stacks. The thermal and geometric properties of the stack are given in Tables I and II.

$$\rho_{\mathrm{s}} c_{\mathrm{s}} \frac{\partial T_{\mathrm{s}}}{\partial t} = k_{\mathrm{s}} \nabla^2 T_{\mathrm{s}}, \tag{4}$$

with subscripts f and s denoting fluid and solid, respectively. The thermal conductivity, k, is assumed constant in time and space. The velocity field is denoted by $\mathbf{u}$, time is denoted by t and the specific heat and mass density are c and ρ, respectively. The two equations, 3-4, are coupled at their interface by assuming continuity. The model is implemented and solved in the commercial software package Comsol v. 4.2 and the details are provided in Ref. [17, 20].

The outlet temperature as a function of time may be used to deduce the bulk heat transfer properties of the heat exchanger. Various techniques may be applied; see, e.g., Ref. [21]. In Refs. [17, 20] the details of the analysis of parallel plate heat exchangers are outlined and discussed. Such an analysis results in the above mentioned Nusselt scaling factor ($\mathrm{Nu}_{\mathrm{scl}}$), which is a function of the flow rate (Reynolds number), stack geometry and thermal properties. In Fig. 2 the $\mathrm{Nu}_{\mathrm{scl}}$ factor is plotted as a function of Reynolds number defined as

$$\mathrm{Re} = \frac{2\rho_{\mathrm{f}} \dot{V}'}{N \mu_{\mathrm{f}}} \tag{5}$$

where μ_{f} is the dynamic viscosity. The thermal and geometric properties are given in Tables I-II. The scaling factor is based on the statistics of 50 stacks each having 20 channels with normally distributed thicknesses. Five different standard deviations have been investigated (5 to 25 % of the mean channel thickness), which is indicated in the figure legend.

Table I. The thermal properties assumed in the flow maldistribution model (thermal conductivity, mass density and specific heat). The values reflect gadolinium (for the solid) and water (for the fluid).

Property	k [W/(m · K)]	ρ [kg/m^3]	c [J/(kg · K)]	μ_f [Pa · s]
Solid	10.5	7900	300	-
Fluid	0.6	1000	4200	0.001

Table II. The geometrical properties of the regenerator considered. The length, L, plate thickness, H_s, and mean channel thickness, $\langle H_\mathrm{f} \rangle$, are kept constant.

Property	L [mm]	H_s [mm]	$\langle H_\mathrm{f} \rangle$ [mm]
Value	40	0.4	0.2

2.2. AMR model

The influence on AMR performance due to inhomogeneity of parallel plate stacks is investigated using a 1D AMR model previously published [19, 22]. The model is well suited for this task since it is possible to directly alter the heat transfer coefficient describing the convective heat transfer between the solid and the fluid. The Nusselt-scaling factor as found above may therefore be directly incorporated into the 1D AMR model.

The AMR model solves two transient partial differential equations describing the heat transfer in the fluid and solid, their thermal interaction and the magnetocaloric effect work input. These equations describe the same fundamental problem as those given in Eqs. 3–4. However, the heat transfer between solid and fluid is modeled with a bulk heat transfer coefficient through the Nusselt number (defined in Eq. 2) and, of course, the magnetocaloric work input term is also included. They may be written as

$$\rho_\mathrm{f} c_\mathrm{f} A_c \epsilon \frac{\partial T_\mathrm{f}}{\partial t} = k_\mathrm{disp} A_c \frac{\partial^2 T_\mathrm{f}}{\partial x^2} - \dot{m}_\mathrm{f} c_\mathrm{f} \frac{\partial T_\mathrm{f}}{\partial x} - a_s A_c \frac{\mathrm{Nu} k_\mathrm{f}}{d_h} (T_\mathrm{f} - T_\mathrm{s}) \tag{6}$$

$$\rho_\mathrm{s} c_\mathrm{s} A_c (1-\epsilon) \frac{\partial T_\mathrm{s}}{\partial t} = k_\mathrm{stat} A_c \frac{\partial^2 T_\mathrm{s}}{\partial x^2} + a_s A_c \frac{\mathrm{Nu} k_\mathrm{f}}{d_h} (T_\mathrm{f} - T_\mathrm{s}) - \rho_\mathrm{s} A_c (1-\epsilon) T_\mathrm{s} \frac{\partial s}{\partial H} \frac{\partial H}{\partial t} \tag{7}$$

The cross-sectional area of the regenerator bed is denoted A_c, the dispersion corrected thermal conductivity of the fluid is k_disp, the mass flow rate of the fluid is $\dot{m}_\mathrm{f}$, the specific surface area of the regenerator solid is $a_s = \frac{2}{H_\mathrm{s}+H_\mathrm{f}}$, the porosity of the regenerator solid is denoted $\epsilon = \frac{H_\mathrm{f}}{H_\mathrm{s}+H_\mathrm{f}}$, the thermal conductivity of the solid is k_stat, the change in entropy of the solid with magnetic field is $\frac{\partial s}{\partial H}$ and the change in magnetic field with time is denoted $\frac{\partial H}{\partial t}$.

The fluid thermal conductivity is corrected for dispersion due to the fluid movement following Ref. [23]:

$$k_\mathrm{disp} = k_\mathrm{f} \frac{\mathrm{Pe}_\mathrm{f}^2}{210} = k_\mathrm{f} \frac{(\mathrm{RePr})^2}{210} = k_\mathrm{f} \left(\frac{\dot{m}_\mathrm{f} d_h c_f}{A_c \epsilon k_\mathrm{f}} \right)^2 \frac{1}{210}. \tag{8}$$

where Pe is the Peclet number and $\mathrm{Pr} = \frac{c_\mathrm{f} \mu_\mathrm{f}}{k_\mathrm{f}}$ is the Prandtl number. The static

conductivity, k_{stat}, is simply

$$k_{\mathrm{stat}} = k_{\mathrm{s}}(1-\epsilon) + k_{\mathrm{f}}\epsilon. \tag{9}$$

The model implementation details may be found in Ref. [19].

The Nusselt number, Nu, is determined as the product of the Nusselt scaling factor, $\mathrm{Nu}_{\mathrm{scl}}$, and the Nusselt number for an ideal parallel plate heat exchanger, $\mathrm{Nu}_{\mathrm{pp}}$. The latter may be found in literature and is a function of the Reynolds number (see Refs. [18, 24] for details). The resulting Nusselt-number that is used as input to the AMR model is then finally:

$$\mathrm{Nu}(\mathrm{Re}) = \mathrm{Nu}_{\mathrm{scl}}(\mathrm{Re})\mathrm{Nu}_{\mathrm{pp}}(\mathrm{Re}). \tag{10}$$

2.3. Magnetic and fluid properties

For simplicity the magnetic field and fluid flow profiles are modeled as step functions such that the magnetic field is applied at the beginning of an AMR cycle and removed at the middle of the cycle (i.e. at time $t = \tau/2$ where τ is the total AMR cycle time). The magnitude of the applied field is 1 tesla and demagnetizing effects are ignored. The fluid flow is likewise set to move from the cold to the hot end in the first half of the AMR cycle and then the reverse in the other half.

The properties of the solid and fluid are assumed constant except for the specific heat of the solid, which is temperature and magnetic field dependent. The magnetocaloric properties and thus also the specific heat of the solid are found using the mean field model for ferromagnets combined with the Debye and Sommerfeld models for the structural contribution to the specific heat [25, 10]. The solid material is assumed to be gadolinium with the relevant properties given in Table I. The heat transfer fluid is assumed to be water with properties also given in Table I.

3. Results and discussion

The AMR performance is investigated as cooling power versus temperature span in the following at different AMR operating frequencies and values of the thermal utilization. The AMR frequency is defined as $f = 1/\tau$ and the thermal utilization describes the ratio of the thermal mass of the fluid moved to the thermal mass of the regenerator solid. That ratio may be formulated as:

$$\varphi = \frac{\dot{m}_{\mathrm{f}} c_{\mathrm{f}}}{2 f m_{\mathrm{s}} c_{\mathrm{s}}}, \tag{11}$$

where m_{s} is the total mass of the regenerator solid. It was shown in Section 2.1 that the Nusselt number is a function of Reynolds number and thus implicitly a function of the mass flow rate and the AMR frequency. A variation of these parameters is thus provided in the following.

However, the central parameter that is varied is the standard deviation of the channel thickness. Six values are applied: one with no standard deviation, i.e. a

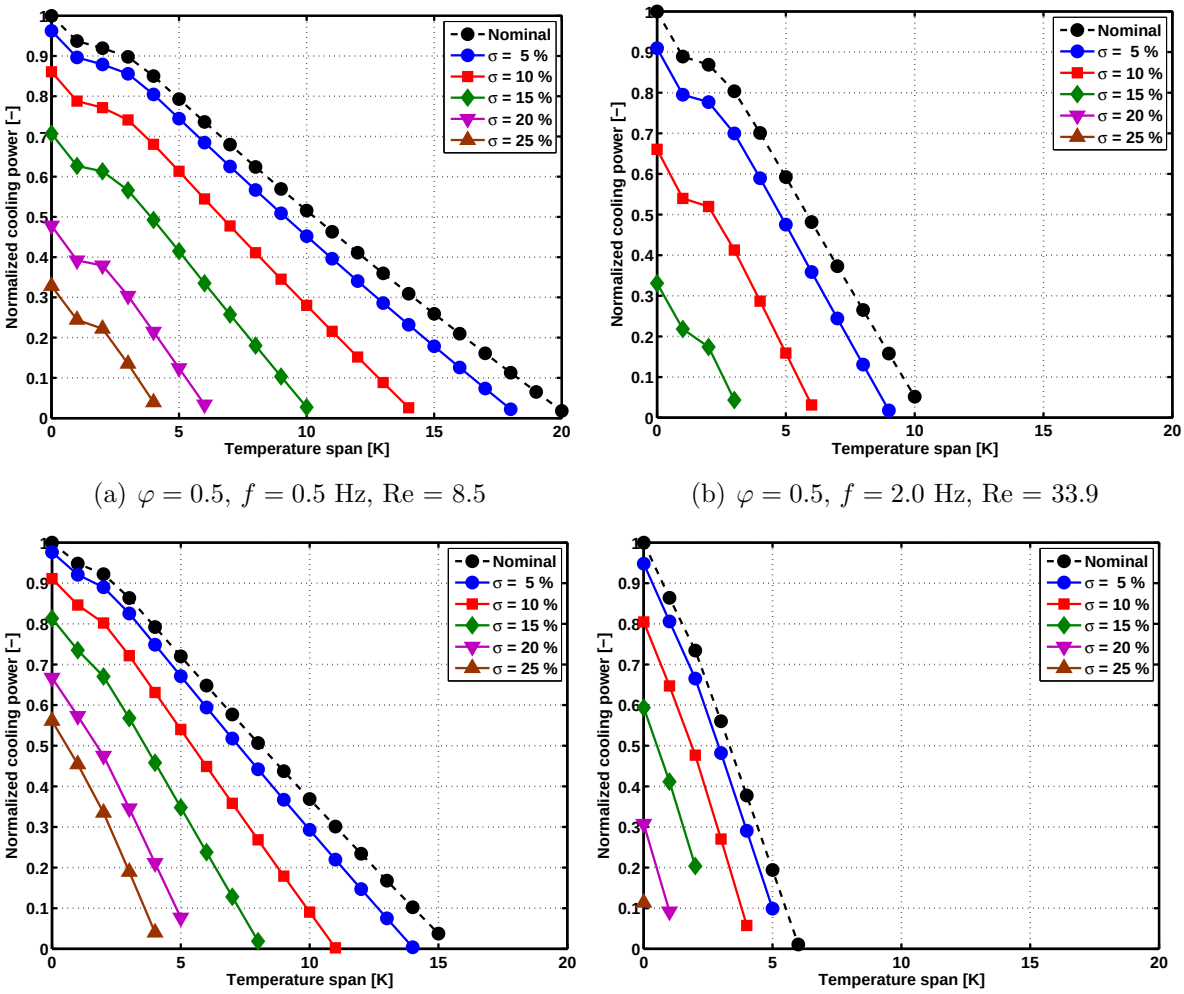

(a) $\varphi = 0.5$, $f = 0.5$ Hz, Re $= 8.5$

(b) $\varphi = 0.5$, $f = 2.0$ Hz, Re $= 33.9$

(c) $\varphi = 1.0$, $f = 0.5$ Hz, Re $= 16.9$

(d) $\varphi = 1.0$, $f = 2.0$ Hz, Re $= 67.8$

Figure 3. (Color online) The normalized cooling power as a function of temperature span ($\Delta T = T_{\text{hot}} - T_{\text{cold}}$). The thermal utilization, defined in Eq. 11, is 0.5 in (a) and (b) and 1.0 in (c) and (d) while the AMR operating frequency is 0.5 Hz in (a) and (c) and 2.0 Hz in (b) and (d). The figure legend indicates the standard deviation of the channel thickness, σ.

benchmark nominal configuration with no flow maldistribution and the five values presented in Fig. 2(b). The hot side temperature was set to 295 K in all the following model cases (the Curie temperature of the mean field modeled Gd assumed as magnetocaloric material was 293 K).

3.1. Cooling power as a function of temperature span

Figure 3 gives the normalized cooling power as a function of temperature span for several combinations of the thermal utilization and AMR operating frequency. For each of these the standard deviation of the channel thicknesses has been varied from zero to 25 % as indicated in the figure legends. The normalization is done for each set of

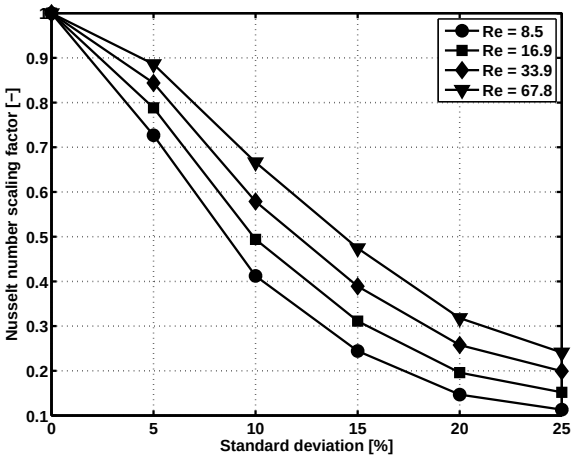

Figure 4. The Nusselt number scaling factor as a function of standard deviation for selected Reynolds numbers

utilization and operating frequency such that the nominal AMR cooling power is one at zero temperature span. All the cooling power values in such a plot are thus divided by the nominal cooling power at zero span.

Generally, the cooling power is linear in the temperature span, which has been reported previously in literature [26, 27]. A slight kink is observed in Figs. 3(a) and 3(b) at a temperature span between one and five K. This is due to the Curie temperature (293 K) and the lower value of the utilization ($\varphi = 0.5$).

From the four plots in Fig. 3 it may generally be concluded that the larger standard deviation on the channel thickness results in decreased AMR performance compared to the nominal situation with a perfect regenerator stack. It is, however, of greater interest to observe that a standard deviation of 5 % does not decrease the performance significantly whereas a standard deviation of 10 % or higher has a very significant impact on the AMR performance.

Considering Fig. 3(a) the maximum achievable temperature span is around 20 K in the nominal case whereas it is only about 4 K for the case with a standard deviation of 25 %. As the utilization or the operating frequency are increased the maximum temperature span decreases. Comparing Figs. 3(a) and 3(c) it may be seen that while the maximum temperature span of the nominal case is decreased from 20 to 15 K the case with a standard deviation of 25 % has virtually no change in maximum temperature span. This difference in behavior is explained from the significant variation of the Nusselt scaling factor as a function of Reynolds number (see Fig. 4).

Comparing Figs. 3(b) and 3(d) (both having an AMR frequency of 2 Hz) it is observed that the cases with standard deviations of 20 and 25 % cannot produce a positive cooling power when the utilization is 0.5 but can at a utilization of 1.0. This is also due to the increase in Nusselt scaling factor as a function of Reynolds number (increasing the utilization at a constant AMR frequency increases the Reynolds number, see Eq. 11).

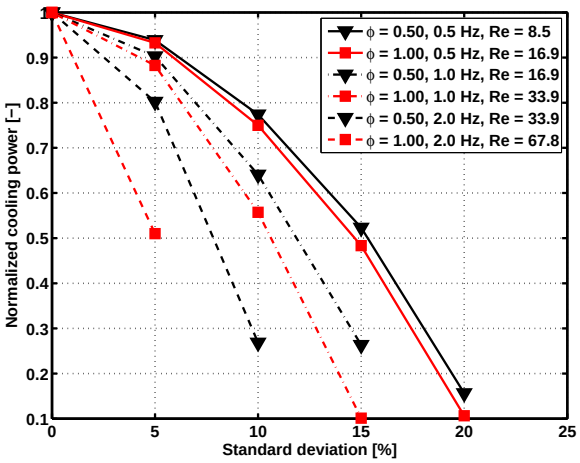

Figure 5. (Color online) The normalized cooling power as a function of standard deviation. The temperature span is fixed at $\Delta T = 5$ K. The legend indicates the thermal utilization, AMR frequency and corresponding Reynolds number. In Fig. 4 the Nusselt number scaling factor as a function of standard deviation for the Reynolds numbers is provided.

3.2. Cooling power as a function of standard deviation

In Figure 5 the normalized cooling power is plotted as a function of standard deviation at different values of the utilization and AMR frequency. Each curve (where the utilization and frequency are constant) is normalized to its respective nominal cooling power, which makes the normalized cooling power equal to one at a standard deviation of 0 %. In order to ensure positive cooling powers the temperature span has been kept constant at $\Delta T = 5$ K for simplicity. Figure 4 shows the Nusselt number scaling factor as a function of standard deviation for the Reynolds numbers considered in Fig. 5.

It is seen from Fig. 5, and hardly surprising, that the cooling power decreases as the standard deviation increases. At a standard deviation of 5 %, however, the decrease is not more than about 10 % to 20 % except for the larger Reynolds number case (Re = 67.8). As the AMR frequency increases the normalized cooling power decreases and as the standard deviation increases the higher frequency (and higher utilizations) cannot sustain a positive cooling power. This is due to two effects.

Firstly, the performance of parallel plates will, in general, decrease at elevated frequencies and/or utilizations (i.e., elevated mass flow rates), since the Nusselt number is virtually constant and thus the heat transfer coefficient is thus approximately constant, which will lower performance at higher flow rates.

Secondly, the increased standard deviation further decreases the Nusselt number, and thus heat transfer coefficient (see Fig. 4). It may thus be concluded that even though the Nusselt number scaling factor increases as a function of Reynolds number (increasing flow rate; see Fig. 2) the resulting performance of heterogeneous stacks of parallel plates is severely lowered compared to the case of the ideal, homogenous stacks.

4. Conclusion

Bulk heat transfer characteristics of heterogeneous heat exchangers of parallel flat plates, previously published, was applied in a detailed one-dimensional numerical AMR model in order to investigate the impact on AMR performance that inhomogeneity of parallel plate AMRs may have.

It was found that above a standard deviation of about 5 % the decrease in cooling power compared to the ideal homogeneous case becomes significant and both the obtainable maximum temperature span (with zero cooling power) and the cooling power at a specific temperature span decrease drastically.

Parallel plate regenerators are often considered in the literature to have interesting properties and to show promise for application in AMRs due to their low flow resistance and, theoretically, large heat transfer coefficients. However, their potential does not seem to have been realized yet (to the knowledge of the present authors) and this may partially be explained from the results provided in this paper.

Finally, it is noted that limits to the tolerances and accuracy in constructing parallel plate heat exchangers have been proved to exist. This may help to guide when building micro channel heat exchangers / regenerators.

Acknowledgements

K.K. Nielsen wishes to thank The Danish Council for Independent Research — Technology and Production Sciences (Contract no. 10-092791) for financial support.

References

[1] J. A. Barclay. Theory of an active magnetic regenerative refrigerator. *NASA Conference Publication*, pages 375–387, 1983.

[2] Vitalij K. Pecharsky and Karl A. Gschneidner Jr. Advanced magnetocaloric materials: What does the future hold? *Int. J. Refrig.*, 29:1239–1249, 2006.

[3] E. Brück, O. Tegus, D.T.C. Thanh, N.T. Trung, and K.H.J. Buschow. A review on mn based materials for magnetic refrigeration: structure and properties. *Int. J. Refrig.*, 31:763–770, 2008.

[4] K. Engelbrecht, K. K. Nielsen, and N. Pryds. An experimental study of passive regenerator geometries. *Int. J. Refrig.*, 34:1817–1822, 2011.

[5] K. Engelbrecht, C. R. H. Bahl, and K. K. Nielsen. Experimental results for a magnetic refrigerator using three different types of magnetocaloric material regenerators. *Int. J. Refrig.*, 30(4):1132–1140, 2011.

[6] N. Pryds, F. Clemens, M. Menon, P. H. Nielsen, K. Brodersen, R. Bjørk, C. R. H. Bahl, K. Engelbrecht, K. K. Nielsen, and A. Smith. A monolithic perovskite structure for use as a magnetic regenerator. *J. Am. Ceram. Soc.*, 94:2549–2555, 2011.

[7] A. Tura and A. Rowe. Permanent magnet magnetic refrigerator design and experimental characterization. *Int. J. Refrig.*, 34:628–639, 2011.

[8] O. Peksoy and A. Rowe. Demagnetizing effects in active magnetic regenerators. *J. Magn. Magn. Mater.*, 288:424–432, 2005.

[9] Kaspar Kirstein Nielsen, Anders Smith, Christian Bahl, and Ulrik Lund Olsen. The influence of

demagnetizing effects on the performance of active magnetic regenerators. *Journal of Applied Physics*, 112:094905, 2012.

[10] T. F. Petersen, N. Pryds, A. Smith, J. Hattel, H. Schmidt, and H.J.H Knudsen. Two-dimensional mathematical model of a reciprocating room-temperature active magnetic regenerator. *Int. J. Refrig.*, 31:432–443, 2008.

[11] K. K. Nielsen, C. R. H. Bahl, A. Smith, R. Bjørk, N. Pryds, and J. Hattel. Detailed numerical modeling of a linear parallel-plate active magnetic regenerator. *Int. J. Refrig.*, 32:1478–1486, 2009.

[12] K. K. Nielsen, J. Tusek, K. Engelbrecht, S. Schopfer, A. Kitanovski, C. R. H. Bahl, A. Smith, N. Pryds, and A. Poredos. Review on numerical modeling of active magnetic regenerators for room temperature applications. *Int. J. Refrig.*, 34:603–616, 2011.

[13] P. V. Trevizoli, J. R. Barbosa, and R. T. S. Ferreira. Design and preliminary results of a gd-based linear reciprocating active magnetic regenerator test apparaturs. In *Fourth International Conference on Magnetic Refrigeration at Room Temperature*, 2010.

[14] K. K. Nielsen, J. R. Barbosa, and P. V. Trevizoli. Numerical analysis of a linear reciprocating active magnetic regenerator. In *Fourth International Conference on Magnetic Refrigeration at Room Temperature*, 2010.

[15] P. Rosa, T.G. Karayiannis, and M.W. Collins. Single-phase heat transfer in microchannels: The importance of scaling effects. *Appl. Therm. Eng.*, 29:3447–3468, 2009.

[16] J. B. Jensen, K. Engelbrecht, C. R. H. Bahl, N. Pryds, G. F. Nellis, S. A. Klein, and B. Elmegaard. Modeling of parallel-plate regenerators with non-uniform plate distributions. *Int. J. Heat Mass Transfer*, 53:5065–5072, 2010.

[17] K. K. Nielsen, K. Engelbrecht, D. V. Christensen, J. B. Jensen, A. Smith, and C. R. H. Bahl. Degradation of the performance of microchannel heat exchangers due to flow maldistribution. *Appl. Therm. Eng.*, 40:236–247, 2012.

[18] M. Nickolay and H. Martin. Improved approximation for the Nusselt number for hydrodynamically developed laminar flow between parallel plates. *Int. J. Heat Mass Transfer*, 45:3263–3266, 2002.

[19] K. Engelbrecht. *A Numerical Model of an Active Magnetic Regenerator Refrigerator with Experimental Validation*. PhD thesis, University of Wisconsin - Madison, 2008.

[20] K.K. Nielsen, C.R.H. Bahl, and K. Engelbrecht. The influence of flow maldistribution on the performance of inhomogeneous parallel plate heat exchangers. *International Journal of Heat and Mass Transfer*, accepted, 2013.

[21] P.J. Heggs and D. Burns. Single-blow experimental prediction of heat transfer coefficients - a comparison of four commonly used techniques. *Experimental Thermal and Fluid Science*, 1:243–251, 1988.

[22] K. Engelbrecht and C. R. H. Bahl. Evaluating the effect of magnetocaloric properties on magnetic refrigeration performance. *J. Appl. Phys.*, 108:123918, 2010.

[23] D. A. Beard. Taylor dispersion of a solute in a microfluidic channel. *Journal of Applied Physics*, 89(8), 2001.

[24] T. F. Petersen, K. Engelbrecht, C. R. H. Bahl, B. Elmegaard, N. Pryds, and A. Smith. Comparison between a 1D and a 2D numerical model of an active magnetic regenerative refrigerator. *J. Phys. D: Appl. Phys.*, 41:105002, 2008.

[25] A. H. Morrish. *The Physical Priciples of Magnetism*. John Wiley & Sons, Inc., 1965.

[26] P. V. Trevizoli, Jr. Barbosa, J. R., and R. T. S. Ferreira. Experimental evaluation of a gd-based linear reciprocating active magnetic regenerator test apparatus. *International Journal of Refrigeration*, 34(6):1518–1526, 2011.

[27] J. Tusek, A. Kitanovski, I. Prebil, and A. Poredos. Dynamic operation of an active magnetic regenerator (amr): Numerical optimization of a packed-bed amr. *Int. J. Refrig.*, 34:1507 – 1517, 2011.